Passive ring resonator method for sensitive inertial rotation measurements in geophysics and relativity

G. A. Sanders, M. G. Prentiss, and S. Ezekiel

Research Laboratory of Electronics, Massachusetts Institute of Technology, Cambridge, Massachusetts 02139

Received August 3, 1981

As part of a program to develop sensitive laser inertial rotation sensors, we have studied the performance of a passive-resonator technique using a 0.7-m × 0.7-m optical cavity. For an averaging time τ of 10 sec, the random drift was 1.1×10^{-2} deg/h, which was consistent with the shot-noise limit for the present setup. For a longer averaging time the random drift was 5.6×10^{-3} deg/h ($\tau = 90$ sec), showing a slight departure from the shot-noise limit. The problems encountered in the present apparatus, as well as those that are critical in the development of much larger resonators for geophysics and relativity applications, are discussed.

Precision measurement of inertial rotation is of much interest in a number of areas, such as navigation, geophysics,[1] and relativity.[2] The geophysical applications include the measurement of the various effects that cause fluctuations in the earth's rotation rate Ω_E, ranging from 10^{-7} to 10^{-9} Ω_E, for example, nutation, precession, wobble, and tidal-friction effects.[1] The relativistic effects range in sensitivity from 10^{-9} to 10^{-11} Ω_E and include measurements of the preferred frame and the drag parameters.[2]

The advent of the laser in 1960 rekindled the interest in the use of the Sagnac effect[3] for sensing inertial rotation by optical means. Several approaches to implementing the Sagnac effect have been under investigation. These include active techniques, such as the ring laser gyro,[4] and passive techniques employing passive ring resonators[5] or multiturn fiber-optic interferometers.[6] In all these approaches, the measurement sensitivity scales with the area enclosed by the light path. Typically, to reach the sensitivity needed to measure the geophysical and relativistic effects mentioned previously, it is necessary to consider areas between 10^2 and 10^4 m^2.

In this Letter, we present preliminary performance data obtained by using the passive-resonator technique employing a square cavity approximately 1 m on a side. In addition, we have identified and studied some of the problems that will be critical to the development of very large resonator rotation sensors of the order of 30 m × 30 m or even greater.

Figure 1 shows the experimental setup. The square resonator, 0.7 m on a side, is formed by two spherical maximum-reflectivity mirrors and two 99%-reflectivity flat mirrors used for coupling into, and out of, the cavity. The cavity mirror mounts are fastened to a super Invar table, and the paths between the mirrors are sealed to minimize airflow. Light from a single-frequency 0.7-mW He–Ne laser is split into two beams, each of which is shifted in frequency by an acousto-optic (A/O) modulator before entering the resonator. The polarization of the light is aligned with one of the polarization axes of the resonator. The beam propagating in the clockwise (cw) direction in the cavity is shifted by (a fixed-frequency) f_1, and the counterclockwise (ccw) beam is shifted by f_2. As described previously,[5,7] the cw resonance of the cavity is automatically locked to $f_0 + f_1$ by means of a primary feedback loop driving a piezoelectrically controlled cavity mirror (f_0 is the laser frequency). The operation of the feedback loop is based on a 32-kHz cavity-modulation rate (f_m) with a peak-to-peak frequency excursion of about 150 kHz to achieve optimum discriminant sensitivity with respect to the 450-kHz cavity linewidth. The output of the cw photodetector (PD#1) is first passed through a notch filter at $2f_m$ before phase-sensitive demodulation in PSD#1. The output of PSD#1 then drives the piezoelectric transducer (PZT) through servo electronics.

The output of the ccw detector (PD#2) is also notch filtered at $2f_m$ and is phase-sensitive demodulated in PSD#2. (To reduce the residual noise that is common to both the cw and the ccw beams, the output of PD#1 is subtracted from that of PD#2.) In closed-loop operation, the output of PSD#2 adjusts f_2 through a voltage-controlled oscillator (VCO#2) to lock $f_0 + f_2$ to the ccw cavity resonance.

In the presence of an inertial rotation rate Ω, the

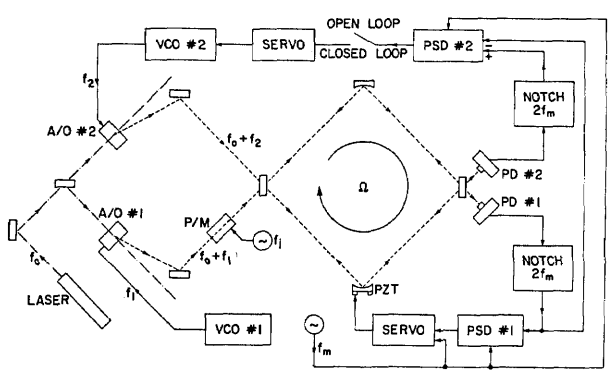

Fig. 1. Schematic diagram of passive ring resonator-rotation sensor.

0146-9592/81/110569-03$0.50/0

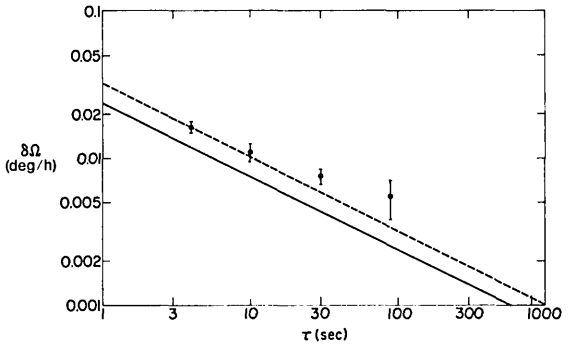

Fig. 2. Random drift error $\delta\Omega$ versus integration time τ.

Sagnac effect, in our case[5] and also for the ring laser gyroscope,[4] reduces to

$$\Delta f = f_2 - f_1 = \left(\frac{4}{\lambda P}\right) \mathbf{A} \cdot \Omega, \tag{1}$$

where A and P are the area and the perimeter of the cavity, respectively, and λ is the wavelength of the light.

The closed-loop drift performance in degrees/hour as a function of averaging time τ, obtained by measuring Δf with a stable frequency counter, is presented in Fig. 2. The random drift was about 1.8×10^{-2} deg/h for an integration time of 4 sec and approximately 5.6×10^{-3} deg/h for an integration time of 90 sec.

The theoretical limit on the uncertainty in measuring Ω, i.e., $\delta\Omega$, is directly related to the uncertainty δf in measuring $f_2 - f_1$, given by

$$\delta\Omega = \left(\frac{\lambda P}{4A}\right) \delta f. \tag{2}$$

For shot-noise-limited detection using the optimum modulation amplitude,[5]

$$\delta f \approx \frac{\sqrt{2}\Gamma}{(N_{\mathrm{ph}} \eta_D \tau)^{1/2}}, \tag{3}$$

where N_{ph} is the average number of photons per second arriving at the detector, η_D is the detector quantum efficiency, τ is the integration time, and Γ is the full width of the cavity resonance at half intensity. The factor $\sqrt{2}$ comes from the incoherent addition of the uncertainties in the measurements of f_1 and f_2. Based on Γ, N_{ph}, and η_D for this apparatus, the photon-noise-limited resolution as a function of τ is depicted by the solid line in Fig. 2. The dotted line represents the effective limit for our present setup, taking into consideration the additional white noise in the detector–preamplifier. As can be seen, the data points are consistent with the shot-noise-limited performance for $\tau \lesssim 10$ sec but depart slightly from the predicted $\tau^{-1/2}$ dependence for $\tau \gtrsim 10$ sec.

Several sources of error are being investigated as possible causes of the long-term drift shown in Fig. 2. For instance, beam misalignment causes excitation of higher-order transverse modes in the cavity that tend to pull the resonance frequency of the TEM_{00} mode that is used as a reference. In this way, unequal cw and ccw beam misalignments generate nonreciprocal frequency errors. To maintain a steady beam alignment we have used stable optical mounts. However, the active components in our setup, i.e., the laser and the A/O transducers, do produce a temperature-dependent beam steering. One possible way to reduce this beam wandering is to employ a single-mode fiber between the A/O modulators and the cavity.

Another source of error arises from the dependence of the effecive resonance frequency of the cavity on the size of the detector and its transverse spatial position with respect to the output beam. This effect, which can influence the cw and ccw beams independently, has been studied carefully, and it has been found that it is caused by improper matching of the input field into the TEM_{00} mode of the resonator.

Yet another important source of error is due to backscattering from the cavity mirrors and scattering in the A/O transducers. Each of these problems results in an oscillatory nonreciprocal frequency shift at the difference frequency $f_2 - f_1$. This effect may be conveniently reduced by putting a phase modulator (P/M) in either beam before cavity injection, as is shown in Fig. 1. If the P/M is driven at a frequency f_j with a sufficient amplitude to suppress the carrier frequency, then the frequency of the oscillatory error signal will be shifted by integer multiples of $\pm f_j$, which can then be removed by appropriate filtering techniques. As an illustration, we purposely injected light from the cw beam into the ccw beam at the input of the cavity, with $f_2 - f_1$ set at approximately 1 Hz. The left-hand portion of Fig. 3 is the open-loop output of PSD # 2, demonstrating the oscillatory error at ~1 Hz. When the phase modulator is driven at $f_j = 4$ kHz, the frequency of this oscillation is shifted by integer multiples of 4 kHz, which are therefore greatly attenuated (right-hand portion of Fig. 3) because they fall well outside the 5-Hz bandwidth of our filter.

The encouraging performance of this intermediate-sized cavity has led us to consider the design of a much larger ring resonator for greater rotation-measurement sensitivity. By inserting the relation $\Gamma \approx (c/\pi P)(1 - R)$, where R is the mirror reflectivity and c is the speed of light, into Eqs. (2) and (3), we obtain

$$\delta\Omega \approx \frac{\lambda c (1 - R)}{\sqrt{8}\pi A (\eta_D N_{\mathrm{ph}} \tau)^{1/2}}, \tag{4}$$

which shows that the fundamental uncertainty in determining Ω is proportional to $A^{-1}(N_{\mathrm{ph}})^{-1/2}$. For example, with a 30-m × 30-m ring resonator and a 4-W laser, it should in principle be possible to reach a sensitivity of $3 \times 10^{-11}\ \Omega_E$ in an integration time of 1 h.

In the development of large resonator-rotation sensors, it is clear that a number of problems will be en-

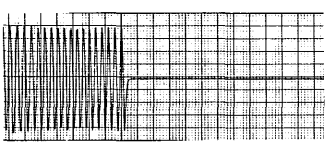

Fig. 3. Oscillatory nonreciprocal frequency shift caused by enhanced backscattering with and without phase modulation.

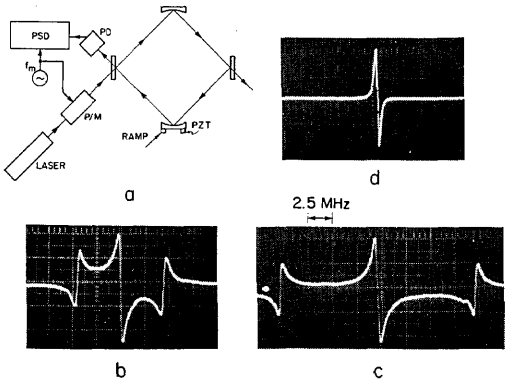

Fig. 4. a, Setup for obtaining discriminant using a phase-modulated laser and detecting the field reflected by the cavity; b and c, resulting discriminants (same vertical scale) obtained for modulation frequency of 4 and 10 MHz, respectively; d, conventional discriminant produced by cavity-length modulation at 32 kHz.

countered. For instance, because a 30-m × 30-m cavity with 99.5%-reflectivity mirrors has a linewidth of the order of 4 kHz, the short-term laser-frequency jitter must be much less than this linewidth. In addition, the laser must have sufficient long-term stability to avoid errors that are due to changes in the scale factor ($4A/\lambda P$). Fortunately, these laser-frequency-related requirements may be achieved by using current stabilization techniques.[8,9] The problem of beam-pointing instabilities caused by the A/O modulators and the laser, which we discussed earlier, are expected to become more important in the case of large resonators. In addition, because of the high sensitivity levels, the cavity itself must be mechanically stable, and the paths between mirrors must be evacuated to eliminate dragging effects. Also, we are studying further the previously mentioned problems attributed to backscattering and the dependence of the cavity-resonance frequency on position and size of the detector. Preliminary calculations indicate that the contributions of these error sources are expected to diminish with increasing cavity size.

A unique and important problem associated with large resonators is that the cavity lifetime, τ_c ($=1/2\pi\Gamma$), is long, and consequently the cavity acts as a filter, which in turn limits the cavity-modulation rate. This rate, however, must be kept sufficiently high (~1 MHz for an argon laser) to ensure that the photon shot-noise limit is the dominant source of noise. In order to produce a discriminant that is independent of τ_c, we have investigated the phase-modulation technique[9] shown in Fig. 4a. Laser light is phase modulated at a rate f_m before injection into the cavity. The reflected, rather than the transmitted, field is detected by the photodetector and is subsequently phase-sensitive demodulated (PSD) at f_m. As an illustration, we phase modulated the laser light at frequencies in excess of the 450-kHz ($= 1/2\pi\tau_c$) linewidth of our 0.7-m × 0.7-m ring cavity. The output of the phase-sensitive demodulator as a function of cavity tuning is shown in Figs. 4b and 4c for modulation rates of 4 and 10 MHz, respectively.

These line shapes, which have sharp dispersivelike features, result from the interference between the carrier frequency and the sidebands as a function of the cavity-resonance frequency. For example, in Fig. 4c the central line shape is a consequence of tuning the cavity resonance over the carrier frequency, and the peripheral features correspond to tuning over the sidebands. In Fig. 4b, because of the lower modulation frequency, these three features partially overlap. A detailed explanation of these line shapes may be found elsewhere.[10] The shape and size of the central discriminant produced by this P/M scheme are similar to those of the conventional discriminant observed in transmission, produced by 32-kHz cavity-length modulation, as is shown in Fig. 4d. In addition, the slopes of the central discriminants in Figs. 4b and 4c are approximately equal to the slope of the discriminant in Fig. 4d. The advantage of the phase-modulation technique over the conventional cavity-length (or laser-frequency) modulation method is that the slope of the discriminant is not significantly affected by the rate of modulation, even if this rate is in excess of Γ. In this way, it is possible to employ the high modulation rates needed to achieve photon-noise-limited detection regardless of the narrow linewidth associated with large resonators.

This research was supported by the U.S. Air Force Geophysics Laboratory.

References

1. M. E. Ash, Charles Stark Draper Laboratory, Inc., Cambridge, Massachusetts (personal communication, December 1976); D. H. Eckhardt, Proc. Soc. Photo-Opt. Instrum. Eng. **157**, 172 (1978).
2. M. O. Scully, in *Proceedings of the Fifth International Conference on Laser Spectroscopy*, H. Walther and K. Rothe, eds. (Springer-Verlag, Berlin, 1979); M. P. Haugan, M. O. Scully, and K. Just, Phys. Lett. **77A**, 88 (1980).
3. E. J. Post, Rev. Mod. Phys. **39**, 475 (1967).
4. A. H. Rosenthal, J. Opt. Soc. Am. **52**, 1143 (1962).
5. S. Ezekiel and S. R. Balsamo, Appl. Phys. Lett. **30**, 478 (1977).
6. V. Vali and R. W. Shorthill, Appl. Opt. **15**, 1099 (1976).
7. S. Ezekiel, J. A. Cole, J. Harrison, and G. Sanders, Proc. Soc. Photo-Opt. Instrum. Eng. **157**, 68 (1978).
8. L. A. Hackel, R. P. Hackel, and S. Ezekiel, Metrologia **13**, 141 (1977).
9. R. V. Pound, Rev. Sci. Instrum. **17**, 490 (1946); R. W. P. Drever and J. L. Hall, Joint Institute for Laboratory Astrophysics, Boulder, Colo. 80309 (personal communication); G. C. Bjorklund, Opt. Lett. **5**, 15 (1980); M. Prentiss, B. Peuse, G. Sanders,and S. Ezekiel, Research Laboratory of Electronics, Progress Report #123, January 1981 (Massachusetts Institute of Technology, Cambridge, Mass.).